

Engine Cycle and Exhaust Configuration for Quiet Supersonic Propulsion

Dimitri Papamoschou*

University of California, Irvine, Irvine, California 92697-3975

The thermodynamics and acoustics of a fixed-cycle, bypass ratio 3 supersonic engine with an innovative noise suppression scheme is explored. The silencing method entails installation of variable turning vanes in the bypass exhaust of a separate-flow turbofan engine. During noise-sensitive segments of flight, the vanes impart a slight downward tilt to the bypass plume relative to the core plume, thus thickening the bypass stream on the underside of the jet. This results in a reduction of the convective Mach number of instability waves that produce intense downward sound radiation. Subscale experiments show that, relative to the mixed-flow exhaust, the coaxial separate-flow exhaust with vanes reduces the peak overall sound pressure level by 8 dB and the effective perceived noise level by 7 dB. The noise-equivalent specific thrust on takeoff is reduced from 490 to 390 m/s. Compared to a current-generation low-bypass turbofan engine, the bypass ratio 3 engine is estimated to be 13 dB quieter with the mixed-flow exhaust and 20 dB quieter with the aforementioned suppression scheme. The vane configuration of this study is estimated to cause a thrust loss of 1% at takeoff and 0.25% at supersonic cruise.

Nomenclature

D	=	diameter
\mathcal{D}	=	drag
F_x	=	axial force of vanes
F_y	=	transverse force of vanes
f	=	frequency
M	=	Mach number
\dot{m}	=	mass flow rate
r	=	distance from jet exit
S	=	planform area of deflector vanes
T	=	thrust
t	=	time from liftoff
U	=	velocity
W	=	weight
x	=	horizontal distance from brake release
y	=	altitude
α	=	geometric angle of attack
γ	=	climb angle
θ	=	polar angle relative to jet centerline
ϕ	=	azimuth angle relative to vertical plane

Subscripts

com	=	compressor
fan	=	fan tip
LO	=	liftoff
p	=	primary (core) exhaust
s	=	secondary (bypass) exhaust
TOM	=	takeoff monitor
tot	=	total
v	=	vanes
∞	=	flight conditions

Introduction

DEVELOPMENT of large-scale supersonic transportation has been a long-sought and elusive goal for the aerospace industry. The efficiency and environmental compliance of a viable supersonic

airplane should be on a par with those of advanced subsonic aircraft. Environmental problems include chemical emissions, sonic boom, and takeoff noise. The latter has been the subject of intense research and development for over 40 years and has led to significant progress in our understanding and prediction of jet noise. A large variety of noteworthy suppression schemes have been proposed and investigated, yet the problem remains as challenging today as it was 40 years ago.¹

At the heart of the issue are the conflicting requirements for an engine that is both quiet on takeoff and efficient at supersonic cruise. Quiet takeoff requires low specific thrust (high mass flow rate). Efficient supersonic cruise entails high specific thrust (low mass flow rate), primarily to minimize the frontal area of the engine. In an effort to resolve this conflict, past efforts have investigated engines with variable-geometry ejectors² as well as turbofan engines with variable cycles (variable bypass ratio). These concepts are notable and are still being pursued, but, at present, entail complexity far greater than that of today's commercial engines.

An ideal concept, of course, would be a fixed-cycle engine that is quiet on takeoff and efficient at cruise. Although this idea was probably unfeasible several years ago, advances in engine technology bring it closer to reality today. A central parameter is the turbine inlet temperature (TIT). As will be shown in the next section, increasing the TIT allows a supersonic engine to operate at higher bypass ratio while maintaining a reasonably small frontal area. Of course, the bypass ratio will never reach the values found in modern subsonic engines, which range from five to nine. Reasonable values for supersonic engines are in the ballpark of two to three; higher values would lead to prohibitively large frontal areas and associated nacelle drag.

This means that noise abatement is still a challenge because the supersonic engine, on takeoff, will have higher specific thrust than its subsonic counterparts. Can an aircraft powered by engines with bypass ratio 3 become as quiet as one powered by engines with bypass ratio 8? The complete answer requires a systems-level view that, at a minimum, considers the following basic and interdependent elements: 1) engine cycle, 2) exhaust configuration, 3) perceived noise (as opposed to absolute noise), and 4) aircraft performance. It is conceivable that optimization at the systems level, and implementation of nontraditional exhaust concepts, will lead to a very quiet supersonic airplane even though the engine has higher specific thrust than its subsonic counterparts.

This study looks at the listed four elements, with emphasis on the effect of exhaust configuration. Given that the bypass ratio is moderate, how one uses the bypass stream to reduce noise becomes crucial. One arrangement is the mixed-flow exhaust, currently used

Received 17 December 2002; revision received 2 September 2003; accepted for publication 10 September 2003. Copyright © 2003 by Dimitri Papamoschou. Published by the American Institute of Aeronautics and Astronautics, Inc., with permission. Copies of this paper may be made for personal or internal use, on condition that the copier pay the \$10.00 per-copy fee to the Copyright Clearance Center, Inc., 222 Rosewood Drive, Danvers, MA 01923; include the code 0748-4658/04 \$10.00 in correspondence with the CCC.

*Professor, Department of Mechanical and Aerospace Engineering, Associate Fellow AIAA.

in all military engines, in which the bypass and core streams mix before exiting a common nozzle. The other option is the separate (unmixed-) flow turbofan, which is very common on subsonic transports. The unmixed design allows shaping of the bypass exhaust so that the bypass stream shields noise emitted from the core stream. Past work on a supersonic engine with bypass ratio (BPR) of 1.6 (Ref. 3) has demonstrated the substantial noise benefit of eccentric separate-flow nozzles. Very recently, alternatives to the eccentric arrangement were developed that make the exhaust arrangement even simpler and allow online control of noise suppression.^{4,5} This paper extends the BPR = 1.6 work to BPR = 3.0 and assesses the impact of the new nozzle configurations.

Engine Cycle

Advances in turbine technology will soon allow steady-state (cruise) operation at TIT around 1800–1900 K. This means that more power will be available to drive a fan with BPR larger than those traditionally used in supersonic turbofan engines (0.5 or less.) Large BPR is desired for quiet takeoff but increases the frontal area of the engine, which is undesirable for supersonic operation. However, at constant thrust, BPR, and fan pressure ratio (FPR), the fan diameter decreases with increasing TIT. Figure 1 plots the variation of fan diameter and thrust specific fuel consumption vs TIT at Mach 1.6 cruise for an engine with BPR = 3.0 and FPR = 2.2. Figure 1 are based on a cycle analysis described later in this section. There is clearly a very significant benefit of a reduced frontal area with increasing TIT. For the conditions shown in Fig. 1, the thrust specific fuel consumption (TSFC) has a minimum of around TIT = 1800 K. Thus, a cruise setting of TIT = 1800 K seems to be a reasonable design point.

Given a turbine inlet temperature in the neighborhood of 1800 K, it is important to know what conditions minimize fuel consumption. The overall pressure ratio (OPR), which, for a supersonic engine,

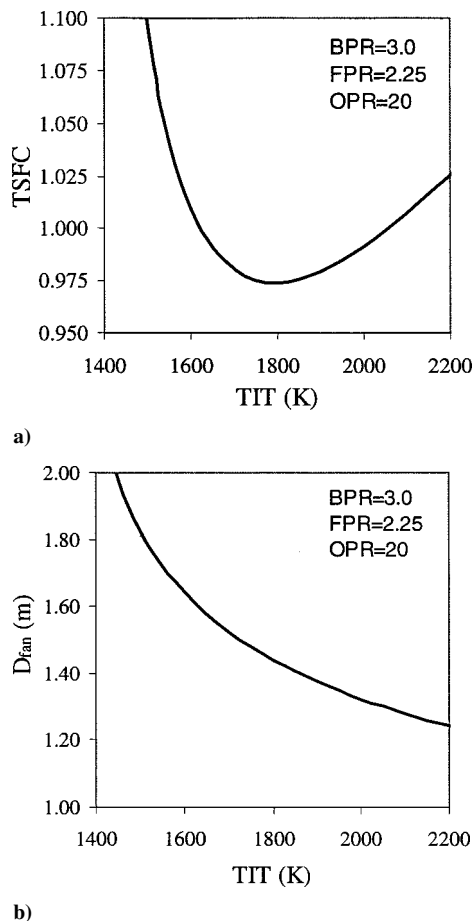


Fig. 1 Engine developing 24-kN thrust at flight Mach number 1.6 variation of a) TSFC and b) fan diameter with turbine inlet temperature.

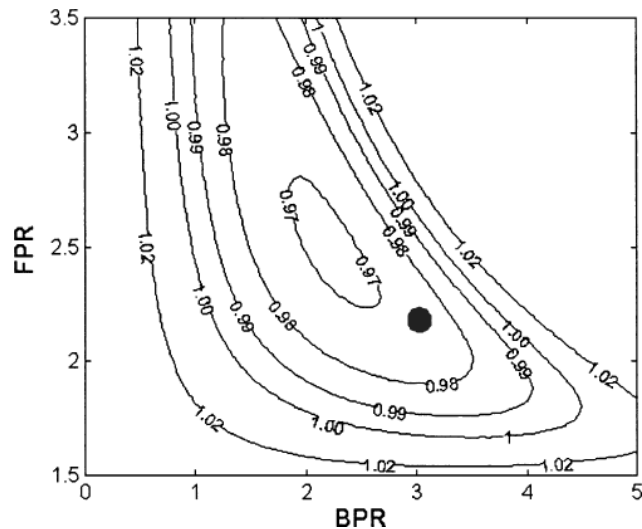


Fig. 2 Isocontours of TSFC on the BPR–FPR plane for $M_\infty = 1.6$; TIT = 1800 K and OPR = 20; dot indicates current design.

should be in the range 15–25, has very slight effect on TSFC. The effects of BPR and FPR are shown in Fig. 2, which plots isocontours of TSFC on the BPR–FPR plane. The minimum TSFC occurs at BPR = 2.2 and FPR = 2.5. What is optimal for cruise, however, may not be the best choice for takeoff. A BPR of 2.2 may be too small for quiet operation. In addition, FPRs above 2.4 will likely require a two-stage fan, which complicates engine design. The selection here is an engine with BPR = 3.0 and FPR = 2.25. As seen in Fig. 2, this condition is very close to the optimum point, yet it increases significantly the chances for meeting noise regulations and affords the simplicity of a single-stage fan.

This study investigates the thermodynamic performance and noise emission from a next-generation BPR = 3.0 supersonic engine with a variety of exhaust arrangements. The exhaust configurations can be broken down into two broad classes, mixed flow and separate flow. For the separate-flow exhaust, nozzle arrangements will comprise coaxial, eccentric, and coaxial with deflectors in the bypass stream. A current-generation supersonic turbofan engine is included in the comparisons to assess the improvements of the new concepts.

To size the engines, we consider a supersonic twin-engine aircraft with a maximum takeoff weight of 540 kN (120,000 lb) and a wing loading of 4450 N/m² (100 lb/ft²). The assumed lift-to-drag ratio is 5 at takeoff and 10 at supersonic cruise, values roughly 20% better than those of the *Aerospatiale Concorde*.⁶ Weight at cruise is 480 kN, based on an average TSFC = 0.6 kg/(kgf · h) and a 20-min climb to cruise altitude. The comparison basis is that all engines have the same cruise thrust at Mach 1.6 and altitude of 16,000 m. On takeoff, the TIT is 200 K greater than the cruise setting, whereas the OPR and FPR values are roughly the same as at cruise. The size, specific fuel consumption, and exhaust conditions are derived from thermodynamic analysis of a Brayton cycle with component efficiencies and specific heat ratios listed in Table 1. (See Ref. 7 for more information on the cycle analysis.) For all of the engines, 25–30% of the compressor air is used for turbine cooling, 1% of the compressor air is bled to systems outside the engine, and 1.5% of the turbine work drives auxiliary systems. Total pressure loss due to turbine cooling is estimated to be 0.07 times the mass fraction of cooling air.⁸ For the mixed-flow designs, the core and fan streams mix at constant pressure, constant total enthalpy, and Mach number 0.4 before expanding to ambient pressure.

Tables 2 and 3 summarize the engine characteristics and thermodynamic performance at supersonic cruise and takeoff, respectively. For convenience, a notation is used that gives the BPR and type of exhaust, for instance, BPR of 3.0 for a mixed-flow engine is B30-MIX. Because of its small BPR, the current-generation engine (B03-MIX) operates at much larger FPR than the B30 variants. Increasing the

Table 1 Engine cycle assumptions

Component	Efficiency	Specific heat ratio
Inlet ($M_\infty < 1$)	0.97	1.40
Inlet ($M_\infty \geq 1$)	0.85	1.40
Fan	0.85	1.40
Compressor	0.85	1.37
Combustor	1.00 ^a	1.35
Turbine	0.90	1.33
Nozzle	0.97	calculation ^b

^aWith 5% total pressure loss. ^bFrom internal mixing calculation.

Table 2 Engine characteristics at supersonic cruise: $y = 16,000$ m, $M_\infty = 1.6$, and $W = 480$ kN

Characteristic	B03-MIX	B30-SEP	B30-MIX
OPR	20	20	20
TIT, K	1600	1800	1800
\dot{m}_{com} , kg/s	44	34	34
\dot{m}_{tot} , kg/s	57	136	136
\mathcal{T} , kN	24	24	24
BPR	0.3	3.0	3.0
FPR	4.5	2.25	2.25
D_{fan}^a , m	0.93	1.44	1.44
TSFC, kg/kgf · h	0.980	0.975	0.974 ^b
M_p	2.06	1.54	1.75
U_p , m/s	890	760	650
M_s	—	1.96	—
U_s , m/s	—	610	—

^a $M = 0.7$ at fan face. ^bDoes not account for mixer losses.

Table 3 Engine characteristics at takeoff: $y = 0$ m, $M_\infty = 0.3$, and $W = 540$ kN

Characteristic	B03-MIX	B30-SEP	B30-MIX
OPR	20	20	20
TIT, K	1800	2000	2000
\dot{m}_{com} , kg/s	120	94	94
\dot{m}_{tot} , kg/s	157	377	377
\mathcal{T} , kN	112	140	145
BPR	0.3	3.0	3.0
FPR	5.0	2.12	2.12
D_{fan}^a , m	0.93	1.44	1.44
TSFC, kg/kgf · h	0.778	0.587	0.565 ^b
M_p	1.55	1.19	1.14
U_p , m/s	770	700	490
M_s	—	1.12	—
U_s , m/s	—	390	—

^a $M = 0.5$ at fan face. ^bDoes not account for mixer losses.

BPR from 0.3 (current generation) to 3.0 (next generation) produces a modest decrease in fuel consumption at supersonic cruise. There is no significant difference between the fuel consumption of the separate-flow and mixed-flow B30 engines. In fact, the actual fuel consumption of B30-MIX may be slightly higher because of losses caused by the mixer. The velocity ratio of the separate-flow exhaust at cruise, $U_s/U_p = 0.80$, is very close to the efficiency of energy transfer between the core and bypass flows (the product of turbine and fan efficiencies, in this case 0.76). This indicates that B30-SEP operates near optimal cruise conditions.⁹

On takeoff, the B30 engines produce substantially more thrust than does the low-bypass reference engine. The thrust-to-weight ratio is 0.5 for the B30-powered aircraft vs 0.4 for the reference case. The resulting initial climb angle,

$$\gamma = \arcsin[(\mathcal{T} - D)/W]$$

is 19 deg for the B30-powered aircraft vs 12 deg for the B03-powered aircraft. The steep climb angle gives the B30-powered aircraft an inherent noise advantage over the reference airplane.

An important consideration in assessing aircraft performance is the weight impact of increasing the BPR from 0.3 to 3.0. A complete

assessment requires detailed systems analysis, which is beyond the scope of this paper. Here we can attempt a very preliminary estimate. A review of the data of commercial and military engines available in the open literature¹⁰ shows that the engine thrust-to-weight ratio is insensitive to BPR and typically ranges between 4 and 6. If a fixed thrust-to-weight ratio of 5 is assumed, the increased thrust of the B30 variants on takeoff translates into roughly 12 kN of extra weight, or 2% of the total aircraft weight. This small penalty can be erased, and even reversed, by advanced technologies that would lead to a lighter engine at the same thrust. The reduced fan stages of the B30 design, combined with the absence of a mixer in the B30-SEP variants, would contribute toward this goal.

Besides engine performance, important information that comes from the cycle analysis includes the exhaust velocities and Mach numbers on takeoff and cruise. The takeoff exhaust conditions are duplicated in subscale tests to assess the acoustics of each configuration. The cruise exhaust conditions are helpful for estimating the thrust loss caused by the vanes during the cruise segment of flight.

Exhaust Configurations

Past research on high-speed jets has shown the powerful noise benefit of reshaping a dual-stream nozzle from coaxial to eccentric.¹¹ Downward-directed Mach wave emission was reduced by the combination of two factors: shortening of the primary potential core (relative to the coaxial jet) and thickening of the secondary flow in the downward direction.¹² This synergism resulted in a reduction of the convective Mach number of flow instabilities that produce intense downward-radiated sound.⁴

Very recent experiments have demonstrated that the overall effect of the eccentric configuration can be achieved in a coaxial jet with deflectors placed in the bypass stream. The deflectors are small flaps, or vanes, that induce a slight downward tilt in the direction of the bypass stream. Flow visualizations⁴ and mean velocity surveys⁵ show that the effect of the vanes is to concentrate the bypass flow to the underside of the jet, near the end of the primary potential core. Absent a secondary flow, the region near the end of the potential core contains the strongest sources of noise.¹³ The vanes create a thick layer of lower speed flow that reduces the relative velocity of the large eddies and, hence, diminishes their ability to radiate noise to the acoustic far field.

Figure 3 shows exemplary illustrations of the separate-flow configurations considered for the B30 engines: coaxial, eccentric, and coaxial with vanes installed in the bypass stream. Figure 4 shows measurements of the mean velocity field in a coaxial jet with and without deflector vanes. For details, the reader is referred to Ref. 5. Even though the flow conditions are not the same as those of the present study, the qualitative trends are expected to be the same. It is seen that the deflection causes a thick layer of bypass flow on the underside of the jet. The deflectors produce superior noise reduction compared to the method of offsetting the nozzles.⁴

Facilities and Flow Conditions

Noise testing was conducted in the University of California, Irvine, (UCI) Jet Aeroacoustics Facility.¹¹ Single- and dual-stream jets with flow conditions matching those given by the cycle analysis (Table 3) were produced. The jets were composed of helium-air mixtures, which duplicate very accurately the fluid mechanics and acoustics of hot jets.¹⁴ Jet nozzles were fabricated from epoxy resin by the use of rapid-prototyping techniques. The nozzles of B03-MIX and B30-MIX were designed with the method of characteristics for Mach numbers 1.5 and 1.2, respectively. For the separate-flow configurations, the primary nozzle was convergent, terminated in a constant-area section, and had a plug along its centerline. All of the primary nozzles had the same exit inner diameter (14.8 mm), lip thickness (0.7 mm), and external shape. The plug diameter was 10.0 mm. One secondary (bypass) nozzle formed a convergent duct in combination with the primary nozzles and terminated in a diameter of 21.8 mm. The pipe that fed the primary nozzle was able to flex, enabling coaxial or eccentric secondary-flow passages. For all of the nozzles, the radial coordinates of the contraction (before any supersonic expansion) were given by fifth-order polynomials. The

Table 4 Flow conditions

Test	Configuration	D_p , mm	U_p , m/s	M_p	D_s , mm	U_s , m/s	M_s
B30-MIX	Mixed flow	14.4	490	1.14	—	—	—
B30-COAX	Coaxial (clean)	10.0 ^a	700	1.19	21.8	390	1.12
B30-ECC	Eccentric	10.0 ^a	700	1.19	21.8	390	1.12
B30-4V20e	Coaxial with four vanes inclined 20 deg, exterior to bypass duct	10.0 ^a	700	1.19	21.8	390	1.12
B03-MIX	Mixed flow (reference)	14.4	770	1.55	—	—	—

^aEffective (area-based) diameter of the primary nozzle; actual dimensions are 14.4-mm i.d. with a 10-mm plug.

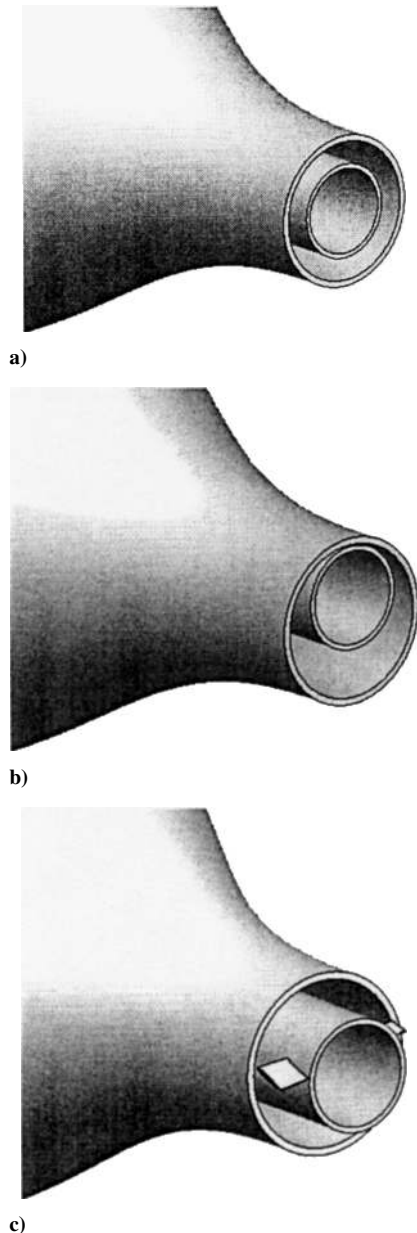


Fig. 3 Separate-flow exhaust configurations considered: a) clean coaxial, b) eccentric, and c) coaxial with bypass deflectors.

contraction ratio was 4:1 for the core nozzles (8:1 with the plug inserted) and 15:1 for the bypass nozzle. The Reynolds number of the primary jet was on the order of 0.5×10^6 . Table 4 summarizes the flow conditions.

Figure 5 shows the B30 nozzle with deflectors attached. The outer wall of the core nozzle extended past the exit of the bypass nozzle. Four vanes, made of thin metal sheet, were attached on the outer wall of the core nozzle immediately past the exit of the bypass nozzle. With $\phi = 0$ indicating the downward vertical direction, the vanes

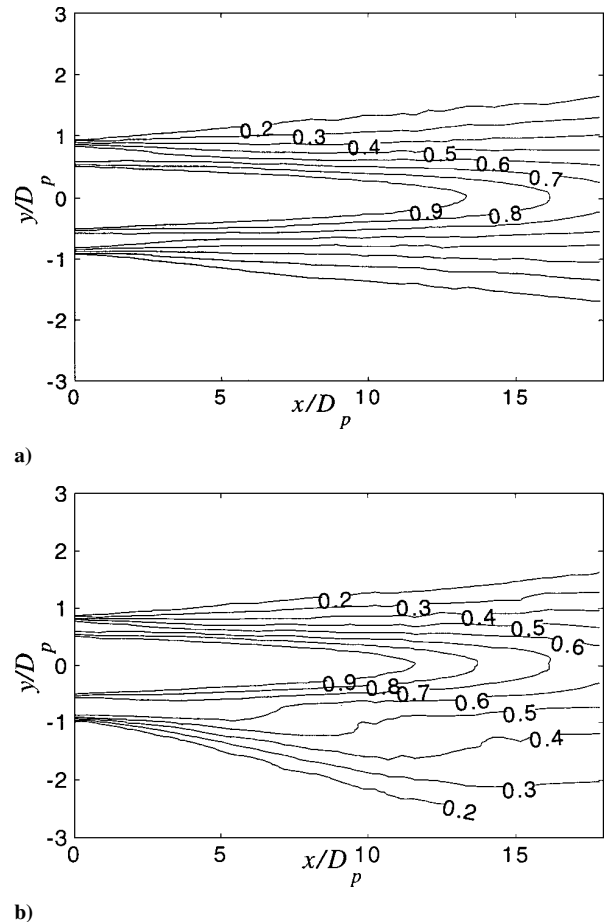


Fig. 4 Isocontours of mean velocity, normalized by U_p , on the plane $\phi = 0$ for a coaxial jet with velocity ratio $U_s/U_p = 0.7$: a) no deflection and b) deflection of the bypass stream (from Ref. 5).

were placed at azimuth angles $\phi = \pm 80$ and ± 110 deg. The vane angle of attack was approximately 20 deg. The size of each vane was 4 mm in chord by 1.7 mm in width. The width was 60% of the annulus thickness of the bypass duct.

Noise measurements were conducted inside an anechoic chamber by the use of a $\frac{1}{8}$ -in. condenser microphone (Brüel & Kjær 4138) with a frequency response of 140 kHz. The microphone was mounted on a pivot arm and traced a circular arc centered at the jet exit with radius of 70–100 core diameters. Earlier experiments have determined that this distance is well inside the acoustic far field.¹⁵ Figure 6 shows the overall setup and the range of polar angles covered. The sound spectra were corrected for the microphone frequency response, free-field response, and atmospheric absorption. Comparison at equal thrust was performed with geometric scaling.¹⁵

Aerodynamic Performance

To estimate the aerodynamic performance of the exhaust with vanes, each vane is treated as a wing with aspect ratio equal to twice the width divided by the chord length. The vane airfoil is

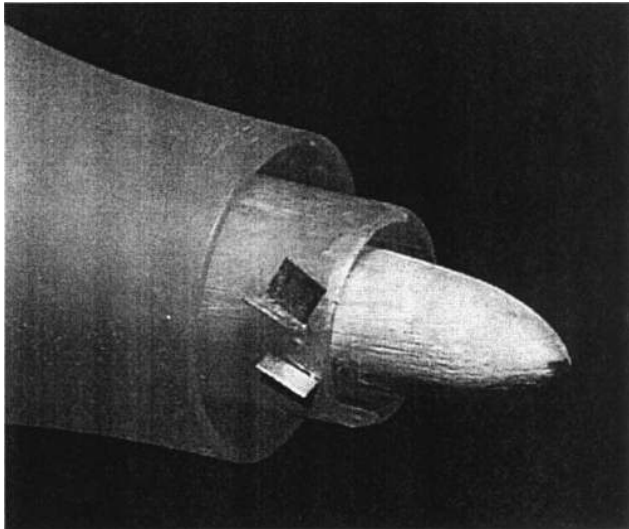


Fig. 5 Nozzle B30-4V20e.

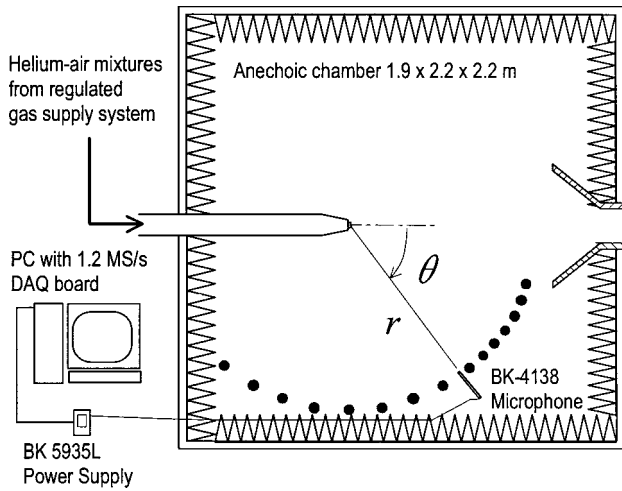


Fig. 6 Experimental setup with set of polar angles covered.

assumed to have zero camber and a thickness-to-chord ratio of 0.06. The relations $T_p = \dot{m}_p(U_p - U_\infty)$ and $T_s = \dot{m}_s(U_s - U_\infty)$ are used in the analysis that follows. When it is assumed that the vanes are situated immediately past the bypass stream exit and that the exhaust is pressure matched, the axial force (drag) on the vanes is

$$F_x = N_v C_D \frac{1}{2} \rho_s U_s^2 S_v$$

where N_v is the number of vanes, S_v is the planform area of each vane, and C_D is the vane drag coefficient. As a fraction of the secondary thrust, the vane drag is

$$F_x/T_s = (N_v C_D/2)(S_v/A_s)[U_s/(U_s - U_\infty)]$$

and the overall thrust loss is

$$\frac{F_x}{T_{tot}} = \frac{N_v C_D}{2} \frac{S_v}{A_s} \frac{U_s}{U_p - U_\infty + \text{BR} \cdot (U_s - U_\infty)} \quad (1)$$

The drag coefficient of each vane comes from the fundamental aerodynamic relation¹⁶

$$C_D = C_{D0} + (C_L^2/\pi \mathcal{R} e) \quad (2)$$

where C_{D0} is the parasite drag, C_L is the lift coefficient, \mathcal{R} is the aspect ratio, and $e \approx 0.8$ is the Oswald efficiency factor. The lift coefficient is given by

$$C_L = \frac{a_{2D}}{1 + 57.3 a_{2D}/(\pi \mathcal{R})} \alpha$$

where $a_{2D} \approx 0.08 \text{ deg}^{-1}$ is the two-dimensional lift slope and α is the angle of attack measured in degrees. In this experiment $\mathcal{R} = 0.8$; hence,

$$C_L = 0.03\alpha$$

Even though the preceding relations are intrinsically subsonic, experiments show that they give reasonable estimates at transonic and supersonic speeds, for example, see Refs. 17 and 18.

At takeoff conditions (Table 3), the vanes were inclined at $\alpha = 20 \text{ deg}$ and, hence, generated a lift coefficient of around 0.6. The freestream Mach number for the vanes was $M_s = 1.14$, for which a fair estimate for C_{D0} is 0.03 (Ref. 18). Equation (2) gives $C_D = 0.2$, which agrees with measurements of drag coefficient in low-aspect-ratio airfoils with $C_L = 0.6$ and Mach number range of 0.8–1.5 (Ref. 17). The vane and nozzle dimensions give $S_v/A_s = 0.15$. For the exhaust conditions shown in Table 3, Eq. (1) predicts a thrust loss of 1.0%.

For flight segments that do not require noise suppression, the vanes would rotate to zero angle of attack or fold into the nacelle structure. Retraction of the vanes into the nacelle would eliminate any thrust loss, but is probably more mechanically complex than rotation of the vanes. Here we examine the thrust loss at Mach 1.6 cruise (Table 2) caused by the vanes at the zero-lift position. The exhaust is now at $M_s = 1.96$, for which a fair estimate of drag coefficient at zero lift is 0.02 (Ref. 18). Note that the nozzle exit areas at cruise are much larger than at takeoff. Because the vane dimensions are constant, the ratio S_v/A_s drops to 0.07. Equation (1) gives an overall thrust loss of 0.25%. These estimates are preliminary and will be followed by computational predictions of the vane forces.

Spectra and Overall Sound Pressure Level

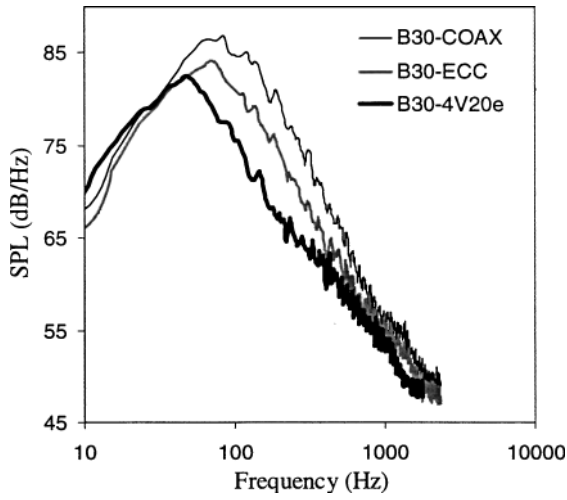
This section discusses the absolute noise levels recorded in the laboratory. These are quantified in terms of the sound pressure level (SPL) spectra and the overall sound pressure level (OASPL). Only the B30 variants are compared; the B03 case is covered in the perceived noise section. The spectra are scaled up to full engine size and referenced to equal thrust. The scale factor (the square root of the ratio of the engine thrust to the calculated laboratory jet thrust³ is 51 for B30-SEP and 92 for B30-MIX. Figure 7a shows a comparison of the spectra in the direction of peak emission of the B30 separate-flow variants. For the low-to-mid-frequencies, the eccentric jet is 5 dB quieter than the clean coaxial jet, whereas the coaxial jet with vanes in the bypass exhaust is 10 dB quieter than the clean coaxial jet. The exhaust with vanes maintains a substantial advantage, of around 10 dB, when compared to the mixed-flow exhaust, as shown in Fig. 7b. In the lateral direction (Fig. 8), the exhaust with vanes is 1–2 dB quieter than the coaxial or eccentric jets and 1–2 dB louder than the mixed-flow configuration.

Even though the separate-flow nozzles were operated with moderate underexpansion, there is no evidence of substantial shock-generated noise. No screech tones or severe increases in broadband noise are evident in the spectra. Because both the core and bypass jets were underexpanded by the same amount, the primary nozzle was actually operating at pressure-matched conditions, at least in the vicinity of its exit. This may have prevented strong waves in the near field of the core jet. The vanes certainly created additional shock/expansion waves in the bypass stream, but Figs. 8 and 9 show that there was no discernible shock noise measured in the far field.

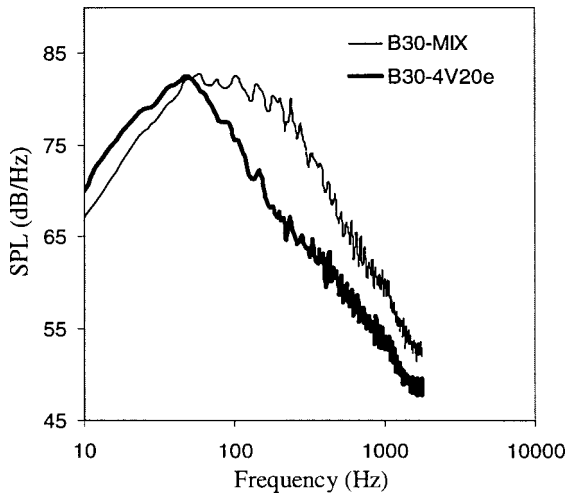
Figure 9 shows a comparison of the directivity of OASPL, at constant thrust and fixed radius from the jet exit, for all of the B30 variants. The advantage of B30-4V20e is again evident: It reduces the peak OASPL by 8 dB relative to the mixed-flow exhaust and by 6 dB relative to the coaxial exhaust. The eccentric arrangement also produces a significant noise benefit, but it is about 2 dB less than the benefit of the coaxial exhaust with vanes in the bypass stream.

Perceived Noise Level

In federal air regulations, aircraft noise is quantified in terms of the effective perceived noise level (EPNL), a metric that incorporates human annoyance to sound and its duration.¹⁹ EPNL thresholds



a)

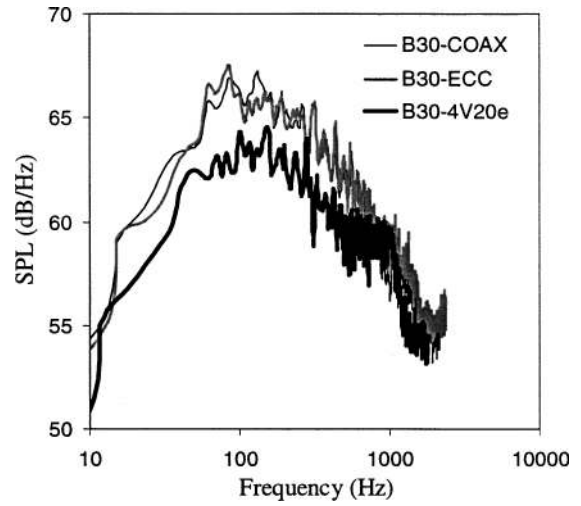


b)

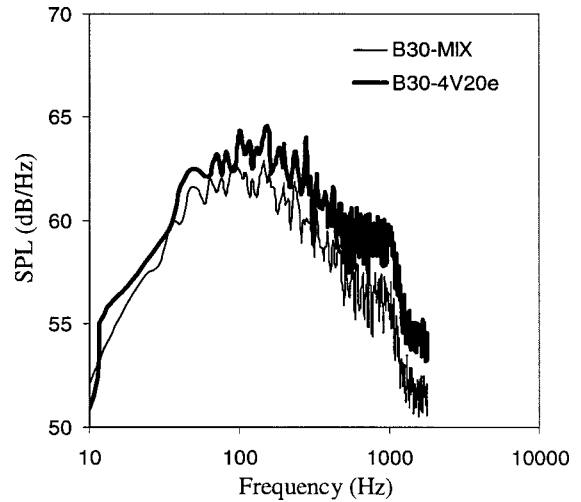
Fig. 7 Far-field, scaled-up spectra in the direction of peak emission ($\theta = 30$ deg) for the B30 variants: a) comparison among the separate-flow variants and b) comparison between B30-4V20e and B30-MIX.

are based on the configuration and weight of the airplane and stem from a mix of scientific and political considerations. Because the ultimate goal of this research is development of quieter airplanes, it is important to obtain estimates of perceived full-scale noise. This is believed to be a meaningful exercise because it includes crucial effects that are typically left out of academic studies of jet noise: distance from the source, atmospheric absorption, and human perception. The absolute levels of EPNL will not be accurate because the effect of forward flight on jet acoustics was not present in the experiments. However, the estimated reduction in perceived noise will provide valuable guidance. Note that other sources of noise, such as fan/compressor and airframe, are obviously not included in this assessment. The emphasis here is on noise recorded from the takeoff monitor for a full-power takeoff. Future studies will address takeoff with power cutback and noise recorded by the sideline and approach monitors.

The first step in assessing perceived noise is definition of the take-off flight path and attitude of the engines relative to the flight path. The airplanes are those defined in the Engine Cycle section, that is, twin-engine with thrust given by the specifications of Table 3. All aircraft must have the same weight because they share the same cruise thrust and the same lift-to-drag ratio at cruise. The flight path of the B30-powered aircraft comprises a takeoff roll $x_{LO} = 1500$ m followed by a straight climb at $\gamma = 19$ deg. The reference B03-powered airplane lifts off at $x_{LO} = 2000$ m and climbs at $\gamma = 12$ deg. For all of the aircraft, the lift coefficient at climb is 0.6, which, for a



a)



b)

Fig. 8 Far-field, scaled-up spectra in the lateral direction ($\theta = 90$ deg) for the B30 variants: a) comparison among the separate-flow variants and b) comparison between B30-4V20e and B30-MIX.

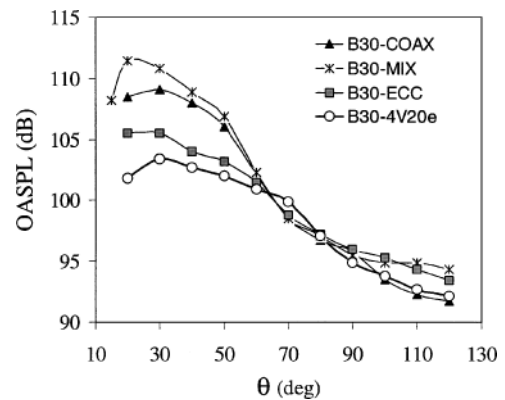


Fig. 9 Directivity of OASPL for the B30 variants.

delta-wing aircraft, corresponds to an angle of attack $\alpha = 12$ deg (Ref. 17). The takeoff flight speed of all airplanes is 110 m/s ($M_\infty = 0.32$). The engine exhaust axis is assumed to be inclined at the angle of attack. Figure 10 shows the generic flight path with key variables.

The steps involved in estimating the time history of perceived noise level [PNL(t)] are described in Ref. 3. The maximum level of PNL (PNLM), is calculated from PNL(t). The duration of PNL

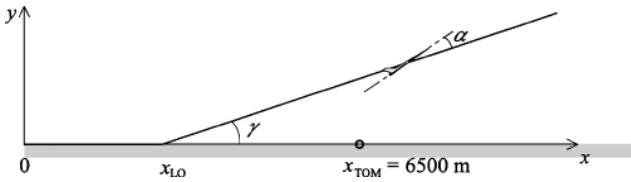


Fig. 10 Flight path used for estimating PNL.

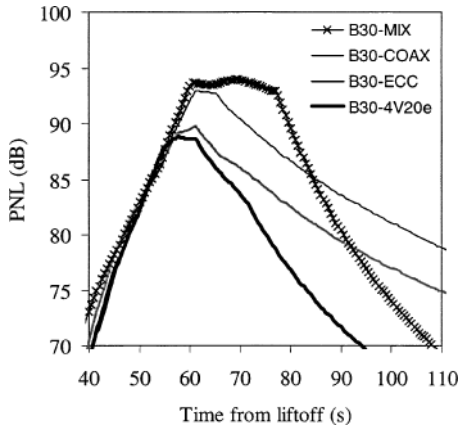


Fig. 11 Time history of flyover PNL of aircraft powered by the B30 variants.

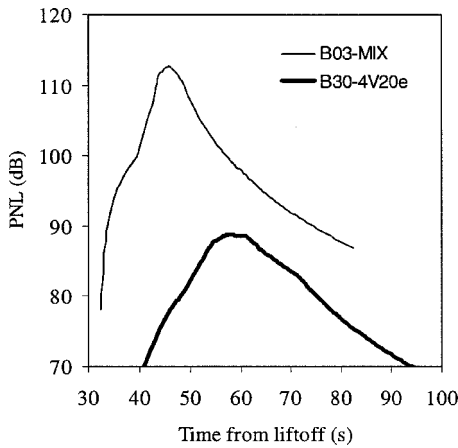


Fig. 12 Time history of flyover PNL for aircraft powered by B03-MIX and B30-4V20e.

exceeding PNL_M -10 dB is calculated, and the corresponding duration correction is computed according to Federal Air Regulations Part 36 FAR 36. The EPNL equals PNL_M plus the duration correction. The estimate of EPNL does not include the tone correction, a penalty for excessively protrusive tones in the one-third-octave spectrum.

Figure 11 shows a comparison of the PNL time histories of aircraft powered by the B30 engine variants. The superiority of the coaxial exhaust with vanes in the bypass exhaust is evident. It lowers the peak PNL by 6 dB and reduces the PNL_M-10 time by 20%. EPNL is as follows: 97.5 dB for B30-MIX 95.5 dB for B30-COAX, 92.0 dB for B30-ECC, and 90.5 dB for B30-4V20e. In other words, the coaxial exhaust with vanes produces a 7-dB benefit in EPNL over the mixed-flow exhaust. Note that the EPNL numbers presented here do not capture the effect of forward flight. Because forward flight reduces all of the velocity differences, the EPNL values at forward flight will be lower than those computed from static conditions. Furthermore, it is expected that forward flight will improve the benefit of B30-4V20e by 1) reducing the convective Mach number of the secondary eddies and 2) reducing the growth rate of the secondary shear layer, thus, stretching the extent of the bypass

flow and providing better shielding of the noise emitted by the core stream. It is hoped that future large-scale experiments will address this issue.

To get an idea of the improvement over current-generation engines, Fig. 12 shows the PNL time history of an aircraft powered by the reference B03-MIX engine and an aircraft powered by the B30-4V20e engine. Recall that the two aircraft have different take-off performance: The one powered by the larger-bypass engine lifts off sooner and climbs at 19 deg vs 12 deg for the reference airplane. The increase in BPR, combined with the new exhaust configuration, gives a 20-EPNLdB noise reduction. This is the ballpark figure cited in numerous studies for bringing noise emission of supersonic aircraft on a par with subsonic aircraft. Note that the traditional exhaust configuration (B30-MIX) produces only a 13-dB benefit relative to the reference case.

Assessment of Noise Reduction

An alternative way to assess noise reduction is to estimate the equivalent exhaust velocity of B30-4V20e as far as noise emission is concerned. To this end, Fig. 13a shows the peak OASPL (scaled to equal thrust and fixed distance from the jet) vs specific thrust of single-stream jets investigated over a period of time in the UCI facility. Overlaid on Fig. 13a is the datum of B30-4V20e. The single-jet data follow the U^8 law very well up to a velocity of 600 m/s, beyond which the growth exponent declines rapidly. Extrapolating the U^8 trend to the OASPL level of B30-4V20e, one finds that the single-stream jet that produces the same noise as B30-4V20e has a

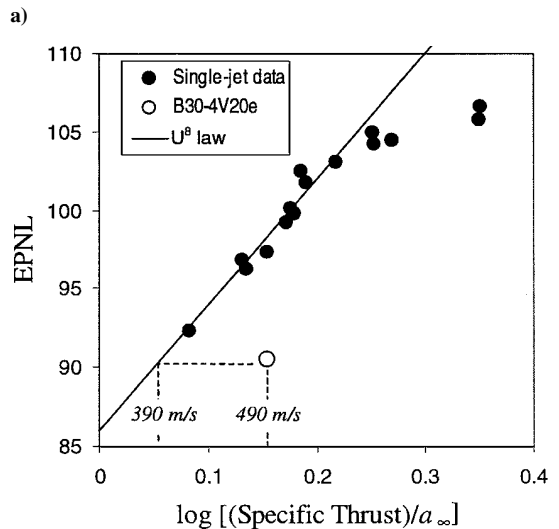
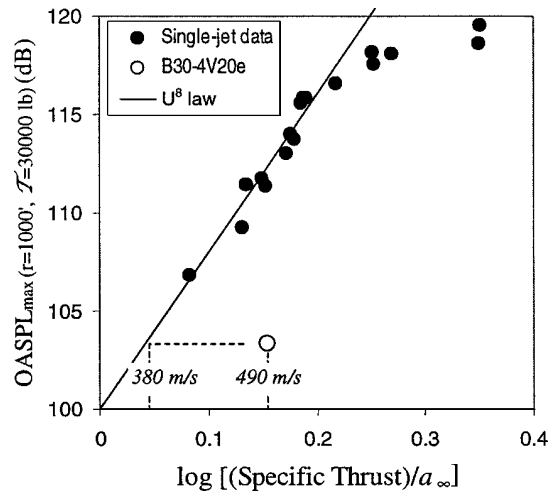


Fig. 13 Comparison of the noise emission of B30-4V20e with those of single-stream jets: a) OASPL and b) EPNL.

velocity of 380 m/s. The effect of the vanes, therefore, was to reduce the noise-equivalent specific thrust from 490 to 380 m/s. Figure 13b shows an analogous comparison in terms of EPNL and leads to a very similar result: The noise-equivalent velocity of the jet is 390 m/s. The exhaust speed range of 380–390 m/s is representative of that found in high-bypass turbofan engines powering subsonic commercial aircraft.

Most important, Figs. 13 illustrate the basic philosophy and paradigm shift of the approach proposed here: suppression of noise via reduction of the convective Mach number while maintained a relatively high exhaust speed is maintained.

Conclusions

The experiments presented demonstrate that it is possible to reduce jet noise significantly while maintaining a high specific thrust. This should help in the development of turbofan engines that are quiet on takeoff and efficient at supersonic cruise. The principle of noise suppression is reduction of the convective Mach number of the turbulent eddies that cause intense downward radiation: The more subsonic the eddies become, the less noise is radiated to the far field.

The preferred implementation of this approach entails installation of variable vanes near the exit of the bypass stream of a separate-flow turbofan engine. During noise-sensitive segments of flight, the vanes would give a slight downward direction to the bypass flow (relative to the core flow), thus, thickening the bypass stream on the underside of the jet. This results in a reduction of the convective Mach number of instability waves that produce intense downward sound radiation. Reductions in downward-emitted noise of 7–8 dB in OASPL and EPNL were measured relative to the mixed-flow exhaust. The vane configuration of this study is estimated to cause a thrust loss of 1% at takeoff and 0.25% at supersonic cruise. A cruise thrust loss of 0.25% appears to fall within the acceptable range for economic operation of an aircraft.

The preliminary cycle analysis presented here suggests that even a BPR = 3.0 supersonic engine would have trouble meeting noise regulations without some kind of suppression scheme. The supersonic cruise requirements lead to an engine with high specific thrust on takeoff, in this case 490 m/s. Implementation of vanes as already noted reduces the noise-equivalent specific thrust (in terms of OASPL or EPNL) to the level of 380–390 m/s. Compliance with noise restrictions would, thus, be greatly facilitated. In addition, the inherently rapid climb of a BPR = 3 powered supersonic airplane will increase the noise compliance margin.

This paper covers one of many possible deflector configurations for tilting the bypass plume. There is a large parameter space to be explored for optimizing the deflectors. In fact, it was recently found that placing the deflectors inside the bypass duct yields acoustic results comparable to those with the deflectors outside.⁵ Such installation has the benefit of a subsonic environment and, hence, alleviation of shock losses and resulting reduction of the drag coefficient of the vanes. Installation of variable vanes will entail some complexity of the engine nacelle, but this appears to be less complex than that of stowable ejector configurations proposed in the past.

Acknowledgments

The support by NASA John H. Glenn Research Center is gratefully acknowledged (Grant NAG-3-2345 monitored by Khairul B. Zaman). Erin Abbey is thanked for her work on nozzle design. The method and apparatus of noise suppression via deflection of the bypass and/or core streams is proprietary to the University of California, U.S. Patent pending.

References

- ¹Smith, M.J.T., *Aircraft Noise*, 1st ed., Cambridge Univ. Press, Cambridge, England, U.K., 1989, pp. 120–134.
- ²Tillman, T. G., Paterson, R. W., and Presz, W. M., “Supersonic Nozzle Mixer Ejector,” *Journal of Propulsion and Power*, Vol. 8, No. 2, 1992, pp. 513–519.
- ³Papamoschou, D., and Debiase, M., “Conceptual Development of Quiet Turbofan Engines for Supersonic Aircraft,” *Journal of Propulsion and Power*, Vol. 19, No. 2, 2003, pp. 161–169.
- ⁴Papamoschou, D., “Noise Suppression in Moderate-Speed Multistream Jets,” AIAA Paper 2002-2557, June 2002.
- ⁵Papamoschou, D., “A New Method for Jet Noise Suppression in Turbofan Engines,” AIAA Paper 2003-1059, Jan. 2003.
- ⁶Mair, W. A., and Birdsall, D. L., *Aircraft Performance*, 1st ed., Cambridge Aerospace Series, Vol. 5, Cambridge Univ. Press, Cambridge, England, U.K., 1992, pp. 260, 261.
- ⁷Debiase, M., and Papamoschou, D., “Cycle Analysis for Quieter Supersonic Turbofan Engines,” AIAA Paper 2001-3749, July 2001.
- ⁸Horlock, J. H., Watson, D. T., and Jones, T. V., “Limitations on Gas Turbine Performance Imposed by Large Turbine Cooling Flows,” *Journal of Engineering for Gas Turbines and Power*, Vol. 123, July 2001, pp. 487–494.
- ⁹Guha, A., “Optimum Fan Pressure Ratio for Bypass Engines with Separate or Mixed Flow Exhaust Streams,” *Journal of Propulsion and Power*, Vol. 17, No. 5, 2001, pp. 1117–1122.
- ¹⁰Mattingly, J., “Aircraft Engine Design,” *Gas Turbine Engine Data*, URL: <http://www.archive.org> [cited 20 August 2003].
- ¹¹Papamoschou, D., and Debiase, M., “Directional Suppression of Noise from a High-Speed Jet,” *AIAA Journal*, Vol. 39, No. 3, 2001, pp. 380–387.
- ¹²Murakami, E., and Papamoschou, D., “Mean Flow Development of Dual-Stream Compressible Jets,” *AIAA Journal*, Vol. 40, No. 6, 2002, pp. 1131–1138.
- ¹³Narayanan, S., Barber, T. J., and Polak, D. R., “High Subsonic Jet Experiments: Turbulence and Noise Generation Studies,” *AIAA Journal*, Vol. 40, No. 3, 2002, pp. 430–437.
- ¹⁴Kinzie, K. W., and McLaughlin, D. K., “Measurements of Supersonic Helium/Air Mixture Jets,” *AIAA Journal*, Vol. 37, No. 11, 1999, pp. 1363–1369.
- ¹⁵Papamoschou, D., and Debiase, M., “Noise Measurements in Supersonic Jets Treated with the Mach Wave Elimination Method,” *AIAA Journal*, Vol. 37, No. 2, 1999, pp. 154–160.
- ¹⁶Shevell, R. S., *Fundamentals of Flight*, 2nd ed., Prentice-Hall, Upper Saddle River, NJ, 1989, p. 187.
- ¹⁷Bertin, J. J., and Smith, M. L., *Aerodynamics for Engineers*, 3rd ed., Prentice-Hall, Upper Saddle River, NJ, 1998, pp. 403–404.
- ¹⁸Ladson, C. L., “Two-Dimensional Airfoil Characteristics of Four NACA 6A-Series Airfoils at Transonic Mach Numbers up to 1.25,” NACA RM L57F05, Aug. 1957.
- ¹⁹“Federal Aviation Regulations Part 36—Noise Standards: Aircraft Type and Airworthiness Certification,” Federal Aviation Administration, Jan. 2002.